Cholesterol and Q147E Deamidation Modulates αA-Crystallin Membrane Binding Elucidating Protective Role of Lens Membrane Composition Changes With Aging

Preston Hazen,[1] Nawal K. Khadka,[2] and Laxman Mainali[1,2]

[1]Biomolecular Sciences Graduate Program, Boise State University, Boise, Idaho, United States
[2]Department of Physics, Boise State University, Boise, Idaho, United States

Correspondence: Laxman Mainali, Department of Physics, Boise State University, 1910 University Drive, Boise, ID 83725, USA; laxmanmainali@boisestate.edu.

Received: December 30, 2024
Accepted: April 14, 2025
Published: May 5, 2025

Citation: Hazen P, Khadka NK, Mainali L. Cholesterol and Q147E deamidation modulates αA-crystallin membrane binding elucidating protective role of lens membrane composition changes with aging. *Invest Ophthalmol Vis Sci.* 2025;66(5):8. https://doi.org/10.1167/iovs.66.5.8

Purpose. The αA-Crystallin (αAc) binding with lens membranes increases with age and cataract formation. However, the role of lipids and cholesterol (Chol) in Q147E-αAc membrane binding remains unclear, which we aim to elucidate in this study.

Methods. We have used the electron paramagnetic resonance spin-labeling method to probe the Chol/ 1-palmitoyl-2-oleoylphosphatidylcholine (POPC) and Chol/ sphingomyelin (SM) membranes binding with wild-type (WT) and Q147E-αAc.

Results. Compared to WT-αAc, the Q147E mutant had increased binding to POPC and decreased binding to SM membranes without Chol. Adding 33 mol% Chol to the POPC and SM membranes decreased the binding of WT and, to a lesser degree, decreased the binding of Q147E-αAc to the membranes. Adding 60 mol% Chol completely inhibited Q147E mutant and WT binding to POPC membranes. However, 33 and 60 mol% Chol completely inhibited WT and Q147E mutant binding to SM membranes, respectively. WT and Q147E-αAc membrane binding decreased membrane mobility while increasing order and hydrophobicity near the headgroup.

Conclusions. In Chol-free membranes, the deamidated Q147E-αAc binds significantly more to the POPC membranes compared to WT, whereas WT binds significantly more to the SM membranes compared to Q147E-αAc. In contrast, for 33 mol% Chol-containing membranes, the deamidated Q147E-αAc binds significantly more to POPC and SM membranes than WT. Conversely, 60 mol% Chol-containing membranes completely inhibit WT and deamidated Q147E-αAc binding to POPC and SM membranes. These results suggest that increased Chol content of the lens membranes during aging protects against accumulation of modified proteins on the membrane associated with cataracts.

Keywords: αA-crystallin (αAc), cholesterol (Chol), cholesterol bilayer domains, electron paramagnetic resonance (EPR) spin-labeling method, cataracts, hydrophobic barrier, percentage of membrane surface occupied (%MSO), binding affinity (K_a), mobility parameter, maximum splitting, hydrophobicity

A cataract is characterized by the buildup of light-scattering high molecular weight (HMW) protein aggregates in the lens, that can associate with the fiber lens cell membrane and diminish eye lens function.[1–8] These HMW protein aggregates are predominantly comprised of the crystallin proteins (α-, β-, and γ-crystallin), which make up approximately 90% of the soluble lens proteins.[4,5,9–13] α-Crystallin (αABc), the primary molecular chaperone of the lens,[5,9,14–17] accounts for an estimated 40% of the total water-soluble lens proteins[9,15,18–23] and exists as polydisperse oligomeric complexes made up of a approximately 3:1 ratio of αA-crystallin (αAc) to αB-crystallin (αBc).[17,24,25] Conversely, β- and γ-crystallin primarily help maintain the structure and refractivity of the lens.[10,13,26] With age, these crystallin proteins have been found to accumulate post-translational modifications (PTMs)[2,7,10,12,19,21,27–36] and bind the eye lens membrane,[5,13,19,31,37,38] which is believed to cause their insolubilization and aggregation into the cataractous light-scattering HMW aggregates.[8,38–41] Relatedly, of these PTMs, deamidation of glutamine (Q) and asparagine (N), which introduces a negative charge at physiological pH, has been shown to alter both crystallin structure and oligomerization and is the most predominant PTM detected in the proteins of cataractous lenses.[2,7,10,21,27,32,33,42] Q147E deamidation of αAc occurs at a significantly higher amount in cataractous lenses relative to that of healthy age-matched lenses,[32,43,44] and has shown to alter the structure of αAc, resulting in a reduced β-sheet content and disruption of the core domain.[44] In addition to deamidation being detected at increased rates in αABc subunits, αABc as a whole has been shown to have the strongest affinity for the lens membrane[14,20,45–51] and becomes increasingly membrane-bound with cataract progression.[6,14,29,45,46,52,53] However, although αABc is found to become increasingly membrane-bound with cataracts[6,14,29,45,46,52,53] and Q147E deamidation of αAc is found at increased levels in cataractous

lenses,[32,43,44] it remains unclear how Q147E deamidation may affect the membrane binding of αAc in cataract development.

In addition to the lens crystallins changing with cataracts, the eye lens membrane lipid and cholesterol (Chol) content has also been shown to change with aging and cataracts. Specifically, with both age and cataract formation, the eye lens shows to increase in its sphingolipids (SLs) content while simultaneously decreasing in phosphatidylcholine (PC) content,[13,26,47,54,55] which is believed to be a mechanism for preventing lens oxidation as SLs have been found to be increasingly resistant to oxidation.[14,56–58] Along this line, we have previously found that the lipid structure (acyl chain length and degree of unsaturation, headgroup, and curvature) also strongly modulates αABc membrane binding, and such binding significantly alters the physical properties of the membranes.[5,59–62] In addition to the lens lipid composition changing with normal healthy aging, the eye lens also significantly increases in Chol content with age.[13,14,26,55,59,63,64] With this high Chol concentration, the eye lens membrane becomes hyper-saturated with Chol, where it forms lipid cholesterol domains (LCDs) and cholesterol bilayer domains (CBDs), with LCDs forming when the membrane becomes saturated with Chol and CBDs forming when Chol concentrations further exceed membrane saturation.[5,59,60,65,66] This uniquely high Chol content has shown to be critical for lens homeostasis, with prior in vivo studies showing that the knockout of lens Chol production in mice results in the development of cataracts,[67] and Tang et al. found Chol significantly decreases the binding of αABc to lipid vesicles.[48] Relatedly in our previous studies, we have found αABc membrane binding to single and dual component membranes,[59,61,62] model lens lipid membranes,[5,60] and membranes made from the isolated cortical or nuclear lipids from single human[55] or bovine lenses,[63] consistently appears to be done through hydrophobic interactions, and these interactions are significantly diminished with the addition of Chol and CBD formation, as Chol decreases hydrophobicity near the membrane surface.[5,55,59,60,62,63] Furthermore, this hydrophobic membrane binding of αABc is believed to possibly form a hydrophobic barrier for the passage of polar molecules and antioxidants, indicating Chol and CBDs likely have beneficial physiological functions in preventing αABc binding and the formation of a hydrophobic barrier, in turn helping to maintain the lens homeostasis and transparency.[5,55,59,60,62,63] However, although studies have been done analyzing the role of lipid and Chol composition on the crystallins membrane interactions, and separate studies have been done analyzing what PTMs are increasingly detected in the membrane-bound crystallins of cataractous lenses, there is minimal research done connecting and understanding how these PTMs affect the lens membrane interactions of the crystallin proteins. Therefore, developing an improved understanding of how the increasingly detected PTMs in cataractous lenses likely alter the modulatory effect of the lens membrane lipid and Chol composition and promote crystallin membrane binding is crucial for understanding the mechanism of cataract formation.

To bridge this gap, we used the electron paramagnetic resonance (EPR) spin labeling method to investigate the membrane interactions of recombinant human wild-type (WT) αAc and Q147E deamidated αAc with Chol/1-palmitoyl-2-oleoylphosphatidylcholine (POPC) and Chol/sphingomyelin (SM*) membranes containing 0, 33, and 60 mol% Chol. This design allows us to see how the deamidation of αAc affects the interactions of αAc with membranes made of the two main lipids found to change in the lens with aging. Simultaneously, we are also able to analyze how the membranes' Chol content before and after CBD formation modulates these αAc membrane interactions with CBD formation taking place at 48 mol% in SM bilayers and 50 mol% in POPC bilayers.[5,65] The results of this study provide new insight into the membrane interactions of αAc, including understanding how αAc differentially interacts with POPC and SM membranes, how Chol and CBDs alter these membrane interactions, how these interactions affect the physical membrane properties (mobility, order, and hydrophobicity), and how Q147E deamidation alters the membrane interactions of αAc.

Materials and Methods

Materials

All of the lipids (POPC, 1-palmitoyl-2-oleoyl-sn-glycero-3-phosphatidylserine [POPS], and SM) and Chol used in this study were obtained from Avanti Polar Lipids, Inc. (Alabaster, AL, USA). HEPES, Tris-HCl, NaN_3, sodium chloride (NaCl), lysozyme, deoxycholic acid, DNase I, and cholestane spin label (CSL) were obtained from Sigma Aldrich (St. Louis, MO, USA). Isopropyl-1-thio-β-D-galactopyranoside (IPTG), ampicillin, phenylmethylsulfonyl fluoride, dithiothreitol (DTT), and polyethyleneimine were purchased from Santa Cruz Biotechnology, Inc. (Dallas, TX, USA). The human WT- and Q147E-αAc genes were developed by and purchased from Genscript USA Inc (Piscataway, NJ, USA) and further expressed, purified, and stored in HEPES buffer (10 mM HEPES, 100 mM NaCl, pH = 7.4) as later discussed. All EPR studies performed analyzing the interactions of αAc (WT and Q147E) with Chol/POPC or Chol/SM* membranes were done in HEPES buffer (10 mM HEPES, 100 mM NaCl, pH = 7.4).

Expression and Purification of Recombinant WT- and Q147E-αAc

WT- and Q147E-αAc were recombinantly expressed using previously described methods in BL21(DE3) *E. Coli* with a pET-43.1a (+) plasmid system.[5,68] Briefly, each plasmid was transformed using the heat shock method into competent *E. coli* BL21 (DE3) and spread on an ampicillin-containing (100 µg/mL) LB agar plate to obtain single colonies for culturing.[69] IPTG (0.5 mM) was then used to induce protein expression through the T7 promoter system. Cells were harvested by centrifugation (5000 × g, 10 minutes, 4°C), resuspended in phenylmethylsulfonyl fluoride (130 µM) and lysozyme (260 µg/mL) containing ice-cold lysis buffer (50 mM Tris-HCl, 100 mM NaCl, pH = 8.0), and incubated for 20 minutes. Following, deoxycholic acid (4 mg per gram of cell pellet) was added to the lysate and shaken for approximately 30 minutes at 37°C before adding 10 µL per gram of original cell pellet DNase I (2 mg/mL) and leaving at room temperature until no longer viscous (approximately 30 minutes). All cell debris was then pelleted by centrifugation (17,000 × g, 15 minutes, 4°C), and the protein containing supernatant was further centrifuged to remove any remaining debris (65,000 × g, 30 minutes, 4°C). DTT (10 mM final concentration) and polyethyleneimine (0.12% final concentration) were then added to the collected supernatant and incubated at room temperature for 10 minutes before again centrifuging (17,000 × g, 10 minutes, 4°C). The super-

natant was collected, dialyzed overnight in Tris buffer (20 mM, pH = 8.5), and filtered through a 0.22 µm syringe filter for purification with the AKTA go protein purification system. The collected WT- and Q147E-αAc were purified using two successive rounds of a two-step chromatography procedure in which anion-exchange chromatography (HiPrep 16/10 DEAE FF column in 20 mM Tris buffer, pH = 8.5, 0–1 M NaCl gradient) was done followed by size-exclusion chromatography (Hiload 16/600 Superose 6 pg gel filtration column in 10 mM HEPES, 150 mM NaCl, pH = 7.4). Following chromatography, the purified human WT- And Q147E-αAc were concentrated by centrifugation (5000 rpm, 4°C) with Amicon Ultra-15 filters and stored at 4°C in HEPES buffer (10 mM HEPES, 100 mM NaCl, pH = 7.4) for use in EPR experiments. WT- and Q147E-αAc purity was confirmed by sodium dodecyl sulfate-polyacrylamide gel electrophoresis (SDS-PAGE), and the concentrations of each were determined by measuring the UV absorbance at 280 nm in triplicate with molecular weights and extinction coefficients estimated using the ProtParam tool on the Expasy server.[70] Last, dynamic light scattering (DLS) measurements were taken with a DynaPro NanoStar (Wyatt Technology Corp., Santa Barbara, CA, USA) using Dynamics software (version 7) for regularization methods to determine the hydrodynamic radius (R_h) and percent polydispersity (%PD) of Q147E-αAc as done in our past works for WT-αAc.[5]

Sample Preparation

For each sample, POPC or SM was mixed with Chol and CSL, with the concentration of CSL in each sample maintained at 2 mol%. Each mixture of lipids, Chol, and CSL was dried to a final volume of approximately 75 µL using a controlled flow of N_2-gas. Following, approximately 360 µL of HEPES buffer (10 mM HEPES, 100 mM NaCl, pH = 7.4) was added to the lipid and CSL mixture before using the rapid solvent exchange method (RSEM) to prepare large multilamellar vesicles (LMVs).[71,72] LMVs then underwent 20 rounds of sonication (10 seconds of sonication followed by 15 seconds of cooling on ice) with a probe-tip sonicator (Fisher Scientific, Model 550) to form small unilamellar vesicles (SUVs), as described in our previous works.[59–61] The prepared SUVs were made of either POPC or SM* (* indicates the presence of 20 mol% POPS and 80 mol% SM) with Chol/lipid mixing ratios 0, 0.5, and 1.5. As mentioned in our previous study,[59] likely due to the strongest affinity of Chol to SM,[73] the preparation of slightly hazy transparent solution of SUVs from sonication of cloudy solution of Chol/SM LMVs could not be obtained even at Chol/SM mixing ratio of 0.1.[59] Therefore, 20 mol% POPS was added to 80 mol% SM to prepare SM* membrane and this molar ratio was maintained when preparing Chol/SM* membranes at mixing ratio of 0, 0.5, and 1.5. As described previously, the preparation of Chol/SM* SUVs becomes more favorable as POPS is a charged phospholipid.[59] Additionally, of all possible phospholipids, POPS is a lipid commonly found in the human eye lens,[56] which is why it was specifically chosen as the charged phospholipid for Chol/SM* SUV preparation. Moreover, to account for any possible effects of POPS, a control experiment was conducted using solely POPS vesicles to investigate the influence of charged phospholipid on the membrane interactions of Q147E and WT-αAc. The prepared SUVs' R_h was determined using DLS for each sample and later used for calculating the percentage of membrane surface occupied (%MSO) by αAc.[5,59,61] Following SUV preparation, the concentration of Chol plus lipids in each sample was maintained at 5.7 mM, and αAc was added at varying concentrations from 0 to 17.9 µM to Chol/POPC membranes and from 0 to 53.8 µM Chol/SM* membranes. HEPES buffer (10 mM HEPES, 100 mM NaCl, pH = 7.4) was added to the αAc and membrane mixtures to a final volume of 70 µL and incubated for 16 hours at 37°C in a shaking incubator (Corning, Corning, NY, USA) to allow for the saturation of αAc membrane binding, as explained in our previous studies.[59,61,74]

EPR Methods

Following incubation, the Chol/POPC and Chol/SM* membranes incubated with WT- or Q147E-αAc were loaded into 1.0 mm internal diameter gas permeable methylpentene polymer (TPX) capillary tubes for the acquisition of EPR measurements at 37°C and −163°C with an X-band Bruker ELEXSYS 500 spectrometer. All EPR measurements were taken with each sample under a constant flow of N_2 gas for deoxygenation and temperature control, and a controlled flow of liquid nitrogen was used to maintain the temperature for measurements taken at −163°C. EPR spectra obtained at 37°C were recorded with an incident microwave power of 8.0 mW and modulation amplitude of 1.0 G, and provided us with the data used to analyze the membrane binding (%MSO, maximum percentage membrane surface occupied [MMSO], and binding affinity [K_a]) of WT- and Q147E-αAc and the effects of αAc binding on the physical properties (mobility and order) of each membrane. All measurements taken at −163°C were recorded with an incident microwave power of 2.0 mW and modulation amplitude of 2.0 G, and used to determine the $2A_z$ value, which is inversely related to and used to measure membrane hydrophobicity. The complete method used to calculate the %MSO by WT- and Q147E- αAc and determine the K_a, mobility parameter, maximum splitting, and $2A_z$ values is described in detail in our previous studies.[13,59,61,74]

Statistics

All collected data describing the interactions of WT- and Q147E-αAc with Chol/POPC and Chol/SM* membranes at mixing ratios of 0, 0.5, and 1.5 are expressed as the mean and standard deviation of the values collected from at least 3 independent experiments. Using the values collected in triplicate for %MSO, K_a, mobility parameter, maximum splitting, and hydrophobicity, a student's *t*-test was done to calculate a *P* value and analyze the statistical significance of each measurement. Unless otherwise stated, a *P* value ≤ 0.05 was considered statistically significant for all experiments.

Results

Membrane Binding of WT- and Q147E-αAc to Chol/POPC and Chol/SM* Membranes

Shown in Figures 1A to 1F is the %MSO by WT- and Q147E-αAc to Chol/POPC and Chol/SM* membranes, with each plotted as a function of protein concentration. As depicted, the %MSO by both WT- and Q147E-αAc to Chol/POPC and Chol/SM* membranes at mixing ratios of 0 (0 mol% Chol) and 0.5 (33 mol% Chol) showed to increase with increasing protein concentrations before becoming constant and saturating at each unique MMSO. For all analyzed samples, the MMSO values followed the trend: MMSO (0 mol% Chol) >

Investigative Ophthalmology & Visual Science

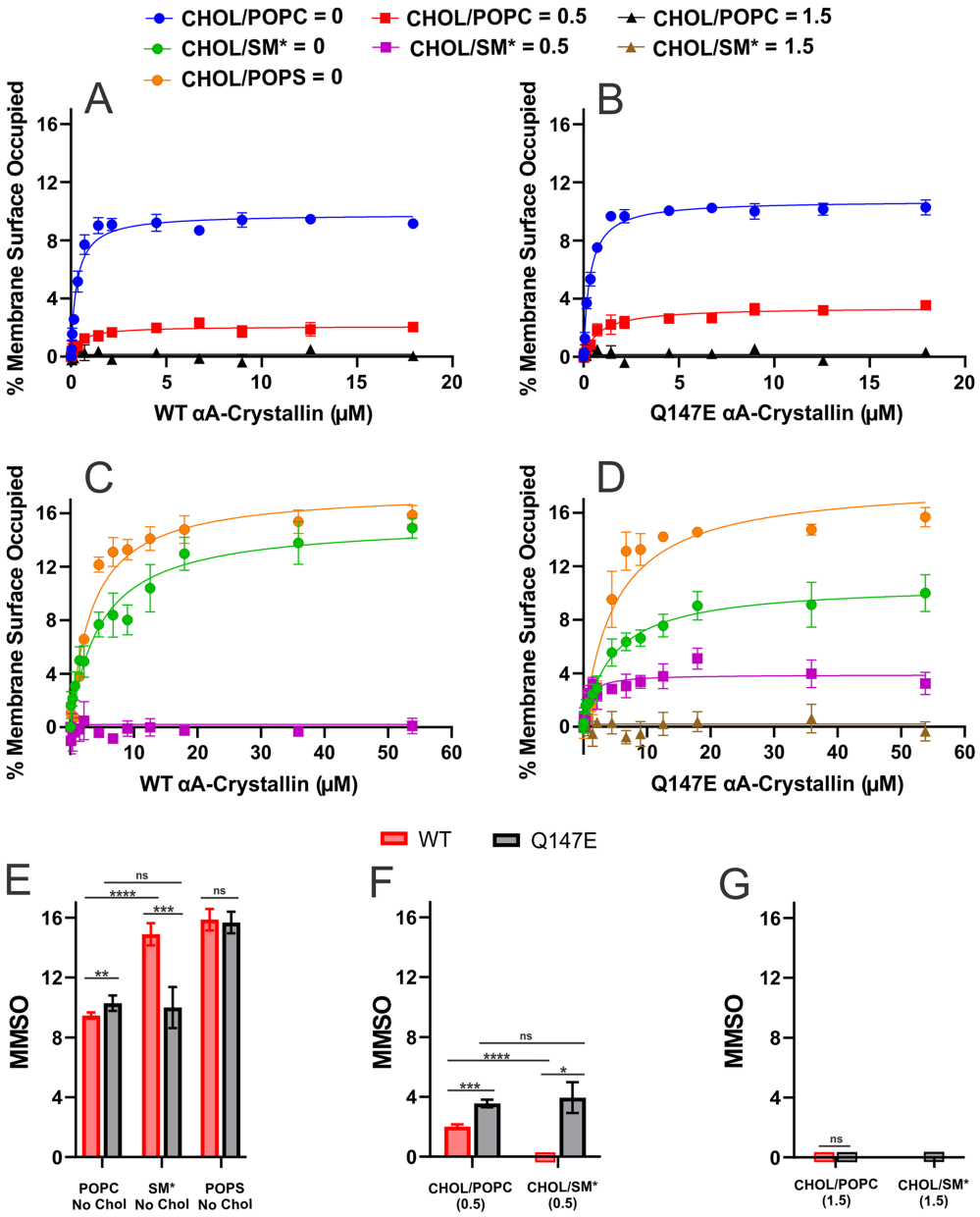

Figure 1. Depiction of the percentage of membrane surface occupied (%MSO) plotted as a function of WT-αAc (**A** and **C**) and Q147E-αAc (**B** and **D**) concentration for Chol/POPC (**A** and **B**), Chol/SM*, and POPS (**C** and **D**) membranes. Shown in **E**, **F**, and **G** are the maximum percentage membrane surface occupied (MMSO) by WT-αAc (*red*) and Q147E-αAc (*black*) to Chol/POPC, Chol/SM*, and POPS membranes at mixing ratios of 0 (**E**), 0.5 (**F**), and 1.5 (**G**). The concentration of lipids plus Chol were maintained at 5.7 mM, while the WT- and Q147E-αAc concentrations were varied from 0 to approximately 18 μM for Chol/POPC membranes (**A** and **B**) and from 0 to 53.8 μM for Chol/SM* and POPS membranes (**C** and **D**). All membranes were incubated with WT- or Q147E-αAc for 16h at 37°C prior to taking EPR measurements at 37°C. The results are the mean ± standard deviation (σ) from at least three independent experiments. *, **, ***, and **** represent a P value < 0.05, < 0.01, < 0.001, and < 0.0001, respectively. Non-statistically significant differences are represented by "ns" for not significant.

MMSO (33 mol% Chol) > MMSO (60 mol% Chol), with the highest MMSO values being found in Chol-free membranes and the addition of Chol continuously resulting in significantly decreased ($P \leq 0.05$) MMSO values until displaying a complete inhibition of binding with the formation of CBDs at a mixing ratio of 1.5 (60 mol% Chol). As depicted in Figures 1A, 1B, and 1E, and 1F for Chol/POPC membranes at mixing ratios of both 0 and 0.5, Q147E-αAc showed to saturate at significantly higher MMSO values ($P \leq 0.05$) than WT-αAc, meaning Q147E deamidation promotes the membrane binding of αAc to Chol/POPC membranes. Interestingly, as displayed in Figures 1C–E in Chol-free SM* membranes, the binding trend is opposite of that seen for POPC membranes, with WT-αAc having a significantly higher ($P \leq 0.05$) MMSO than that found for Q147E-αAc (see Fig. 1F). Moreover, as displayed in Figures 1C–E in the control experiments analyzing the effects of POPS on the membrane binding of WT- and Q147E-αAc, as the SM* membranes are comprised of 20% POPS, there was no significant difference in POPS membrane binding between WT-

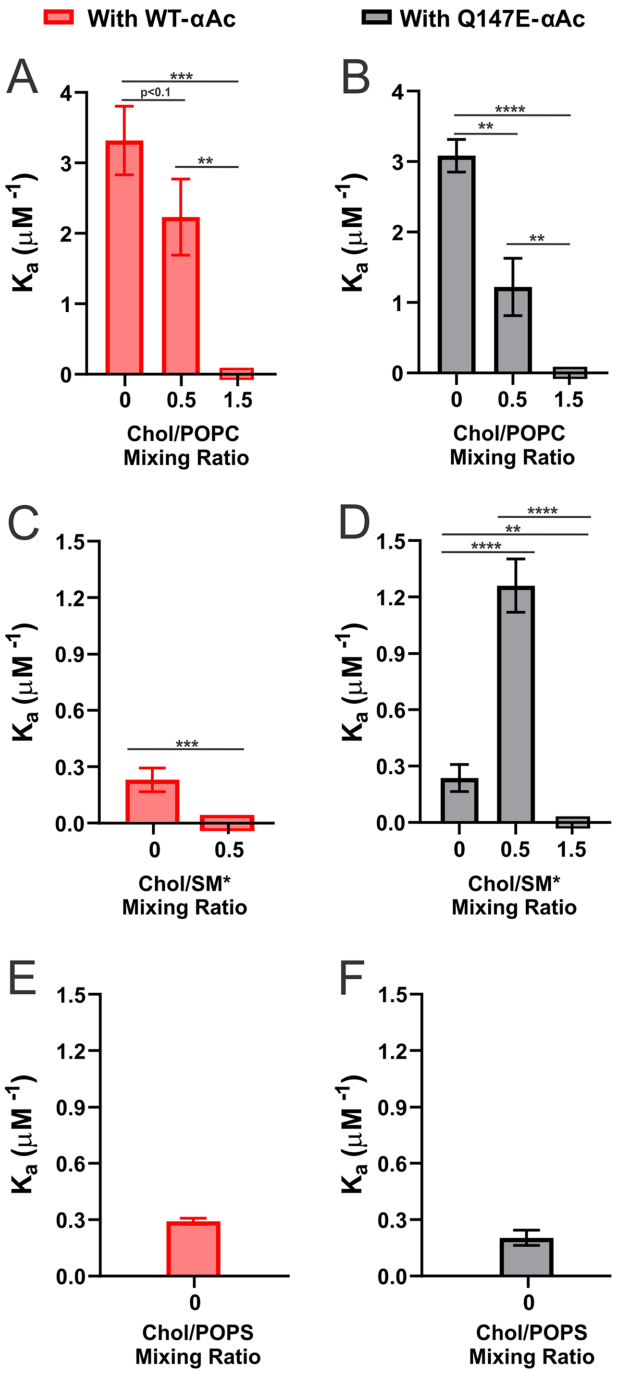

Figure 2. Depiction of binding affinities (K_a) of WT-αAc (**A** and **C**) and Q147E-αAc (**B** and **D**) to Chol/POPC membranes (**A** and **B**), Chol/SM* (**C** and **D**), and POPS membranes (**E** and **F**). As seen in **A** and **B**, with each increase in Chol content, there was a significant decrease in the K_a of WT- (**A**) and Q147E-αAc (**B**) to Chol/POPC membranes until both showed no binding and, in turn, no binding affinity at a Chol/POPC ratio of 1.5. Furthermore, as displayed in **C** and **D** to Chol/SM* membranes, WT- and Q147E-αAc had similar K_a at a mixing ratio of 0, but at a mixing ratio of 0.5, WT-αAc (**C**) showed to have a significant decrease in affinity and no longer displayed any binding, whereas Q147E-αAc (**D**) uniquely showed a significant increase in K_a with an increase in Chol/SM* mixing ratio before again displaying a significant decrease in affinity at a mixing ratio of 1.5, where no binding was detected. As shown in **E** and **F**, WT- and Q147E-αAc had a similar affinity to Chol-free POPS membranes as they did for Chol-free SM* membranes; however, WT-αAc had a significantly higher K_a to these POPS membranes than Q147E-αAc. WT- and Q147E-αAc K_a were estimated by fitting the data points in Figure 1 for WT-αAc (Figs. 1A and 1C) and Q147E-αAc (Figs. 1B and 1D) with a one-site ligand binding model in GraphPad Prism (San Diego, CA). The results are the mean ± standard deviation (σ) from at least three independent experiments. **, ***, and **** represent a P value < 0.01, < 0.001, and < 0.0001, respectively. Changes with a P value between 0.05 and 0.1 are depicted as $P <$ 0.1, and non-statistically significant differences are represented by "ns" for not significant.

and Q147E-αAc indicating the presence of POPS does not influence these SM* membrane binding results. Furthermore, with the addition of Chol at a Chol/SM* mixing ratio of 0.5, the membrane binding of WT- and Q147E-αAc are both significantly decreased ($P \leq 0.05$); however, WT-αAc binding becomes completely inhibited while Q147E-αAc still shows to bind, resulting in Q147E-αAc now having a significantly higher ($P \leq 0.05$) MMSO than WT-αAc (see Fig. 1F). Therefore, in Chol-free SM* membranes, Q147E deamidation diminishes the membrane binding of αAc, but with the addition of 33 mol% Chol, Q147E deamidation reduces the inhibitory effect of Chol and promotes the membrane binding of αAc. Furthermore, in the absence of Chol, WT-αAc has a significantly higher ($P \leq 0.05$) MMSO in Chol/SM* membranes than in Chol/POPC membranes, but at a mixing ratio of 0.5, WT-αAc has a significantly higher ($P \leq 0.05$) MMSO in Chol/POPC membranes than in Chol/SM* membranes. Interestingly, whereas WT-αAc binding significantly changes between each membrane type (POPC versus SM*), Q147E-αAc shows similar MMSO values with no statistically significant difference ($P \leq 0.05$) in both Chol free (0 mol%) and in Chol-containing (33 and 60 mol%) Chol/POPC and Chol/SM* membranes. These variances in membrane binding are likely primarily due to the variances in αAc structure and oligomerization between WT- and Q147E-αAc, where Q147E deamidation disrupts the core domain and reduces β-sheet content.[44] The average R_h of 7.925 ± 0.47 nm estimated for Q147E-αAc in this study is slightly decreased than the previously estimated average R_h of 8.18 ± 0.48 nm for WT-αAc,[5] however, this decrease is not statistically significant ($P > 0.05$). Nevertheless, the average %PD of 21.09 ± 5.28% estimated for Q147E-αAc in this study increases than the previously estimated average %PD of 15.74 ± 5.03% for WT- αAc[5] and this increase is statistically significant ($P \leq 0.05$). Therefore, WT-αAc binding shows to be modulated by both the lipid and Chol composition, whereas likely due to the structural and oligomeric changes, Q147E deamidation diminishes the modulatory effect of lipid type on αAc membrane binding and shows to make Chol and CBD content the primary regulator of αAc membrane binding.

Binding Affinity of WT and Q147E αAc to Chol/POPC and Chol/SM* Membranes

As depicted in Figures 2A and 2B, both WT-αAc and Q147E-αAc showed the highest K_a to Chol-free POPC membranes. Furthermore, with the addition of 33 mol% Chol in Chol/POPC membranes, the K_a of Q147E-αAc significantly decreased ($P \leq 0.05$), whereas the K_a of WT-αAc also showed a decrease that was less pronounced and only significant with $P \leq 0.1$ ($P = 0.0594$). This trend was further pronounced with the addition of 60 mol% Chol where CBDs begin to form, with both WT-αAc and Q147E-αAc showing significant reductions ($P \leq 0.05$) in K_a and no longer having

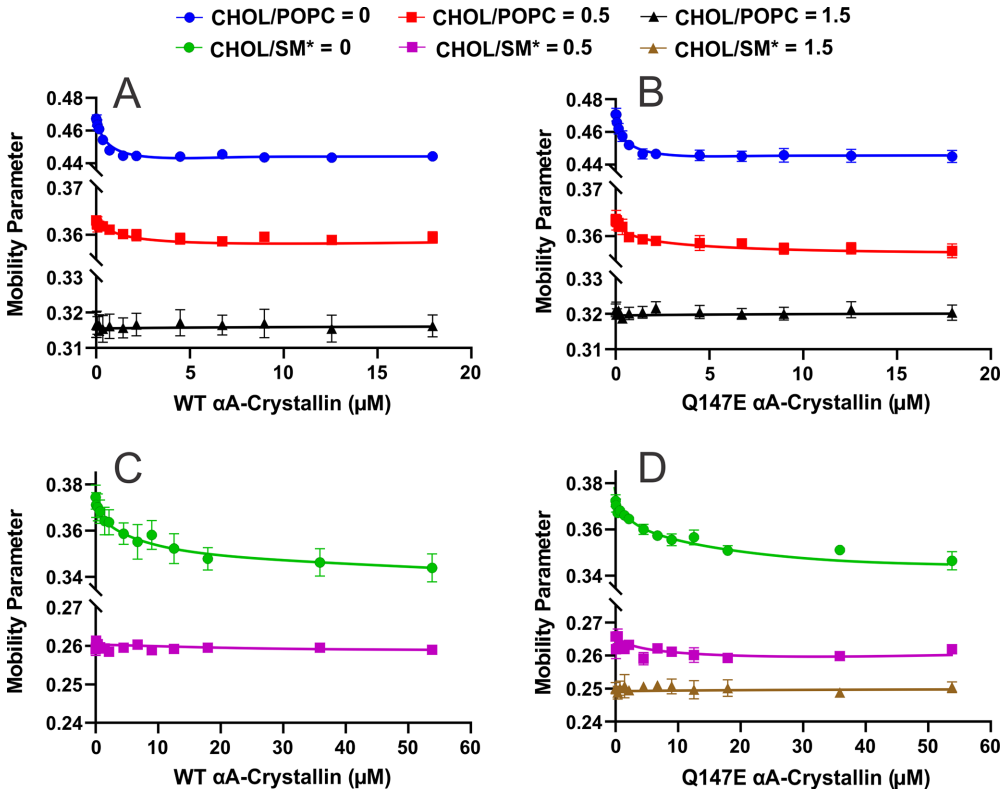

Figure 3. Mobility parameter (h_+/h_0) profiles (membrane mobility near the headgroup region) acquired at 37°C for Chol/POPC (**A** and **B**) and Chol/SM* (**C** and **D**) membranes at Chol/lipid mixing ratios of 0 (*blue* and *green*), 0.5 (*red* and *purple*), and 1.5 (*black* and *brown*) plotted as a function of WT-αAc (**A** and **C**) and Q147E-αAc (**B** and **D**) concentrations. As shown in **A** and **B** for Chol/POPC membranes with each increase in Chol content there is a significant decrease in control membrane mobility, and the binding of WT-αAc and Q147E-αAc at Chol/POPC mixing ratios of 0 (*blue circle*) and 0.5 (*red square*) resulted in significant overall decreases to membrane mobility, but at a mixing ratio of 1.5 no protein binding was detected and therefore there was no change in membrane mobility. As shown in **C** and **D** for Chol/SM* membranes, with each increase in Chol content, there is a significant decrease in control membrane mobility. The binding of WT-αAc and Q147E-αAc at Chol/SM* mixing ratios of 0 (*green circle*) and binding of Q147E-αAc at Chol/SM* mixing ratios of 0.5 (*purple square*) resulted in significant overall decreases in membrane mobility. However, at a Chol/SM* mixing ratio of 0.5 for WT-αAc and 1.5 for Q147E-αAc, no protein binding was detected, and, therefore, no change in membrane mobility was detected. All results are the mean ± standard deviation (σ) from at least three independent experiments.

any affinity (see Figs. 2A, 2B) to Chol/POPC membranes. Furthermore, in Chol-free SM* membranes, there was no significant difference ($P \leq 0.05$) in K_a between WT- and Q147E-αAc; however, both displayed K_a values significantly lower ($P \leq 0.05$) than that found for each protein with Chol-free POPC membranes. Additionally, as shown in Figures 2E and 2F, it is important to note in the control POPS experiments, whereas similar to that found for SM* membranes, WT-αAc had a significantly higher K_a than Q147E-αAc to Chol-free POPS membranes, so the presence of 20% POPS may have a slight effect on increasing the K_a of WT-αAc to the SM* membranes. Furthermore, with the addition of 33 mol% Chol to the Chol/SM* membranes, there was a significant increase ($P \leq 0.05$) in the K_a of Q147E-αAc, while WT-αAc K_a significantly decreases ($P \leq 0.05$) and no longer shows any membrane affinity (see Figs. 2C, 2D). The increase in K_a for Q147E-αAc with the addition of 33 mol% Chol is the only sample that displays an increased K_a with an increase in Chol content, which is likely because the reduced membrane binding found with increased Chol allows for faster binding saturation and, in turn, increases the relative K_a. Furthermore, with the formation of CBDs at a Chol/SM* mixing ratio of 1.5, the membrane binding of Q147E-αAc was completely inhibited and, therefore, displayed no affinity to the membranes (see Fig. 2D). Therefore, these data ultimately show that the binding of WT- and Q147E-αAc is strongest to the Chol-free POPC membranes, and the addition of Chol progressively reduces their strength of binding. Conversely, the addition of Chol shows to differentially impact the K_a of WT- and Q147E-αAc in Chol/SM* membranes, with Q147E deamidation diminishing the inhibitory effect of Chol on the K_a of αAc to Chol/SM* membranes.

Membrane Mobility Near the Headgroup Region of Chol/POPC and Chol/SM* Membranes With WT and Q147E αAc Binding

Displayed in Figures 3A to 3D are the mobility parameters, a measure of membrane mobility near the headgroup region, of WT- and Q147E-αAc to Chol/POPC (see Figs. 3A, 3B) and Chol/SM* (see Figs. 3C, 3D) membranes plotted as a function of protein concentration. As shown, the mobility parameters of Chol/POPC membranes at mixing ratios of 0 and 0.5 show to significantly decrease ($P \leq 0.05$) with increasing concentrations of WT- (see Fig. 3A) and Q147E-αAc (see Fig. 3B), indicating that protein binding

Investigative Ophthalmology & Visual Science

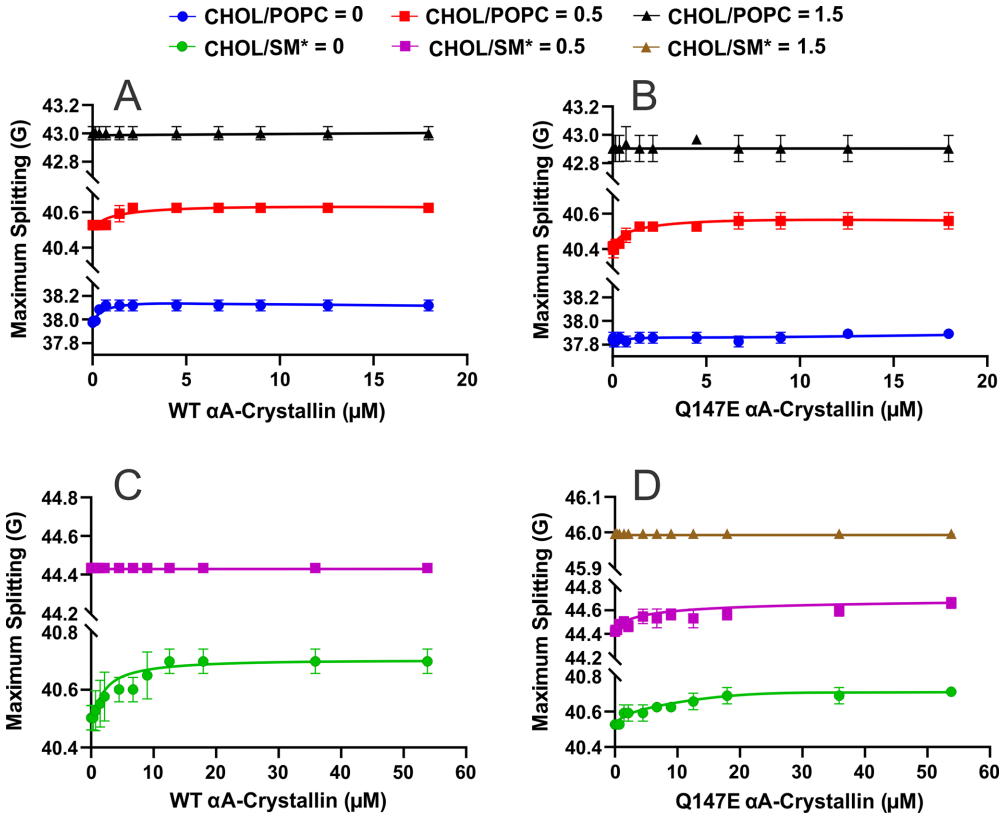

Figure 4. The maximum splitting (membrane order near the headgroup region) profiles obtained at 37°C for Chol/POPC (**A** and **B**) and Chol/SM* (**C** and **D**) membranes at Chol/lipid mixing ratios of 0 (*blue* and *green circles*), 0.5 (*red* and *purple squares*), and 1.5 (*black* and *brown triangles*). All maximum splitting data are plotted as a function of WT-αAc (**A** and **C**) and Q147E-αAc (**B** and **D**) concentrations. As shown in **A** and **B** for Chol/POPC membranes, with each increase in Chol content, there is a significant increase in control maximum splitting. Moreover, the binding of WT-αAc and Q147E-αAc at Chol/POPC mixing ratios of 0 (*blue circle*) and 0.5 (*red square*) resulted in significant overall increases in maximum splitting, but at a mixing ratio of 1.5 no protein binding was detected, and therefore, there was no change in membrane order. As shown in **C** and **D** for Chol/SM* membranes, with each increase in Chol content, there is a significant increase in control membrane order, and the binding of WT-αAc at a Chol/SM* mixing ratio of 0 (*green circle*) and Q147E-αAc at Chol/SM* mixing ratios of 0 (*green circle*) and 0.5 (*purple square*) resulted in significant overall increases in membrane order. However, no protein binding was detected at a mixing ratio of 0.5 for WT-αAc and 1.5 for Q147E-αAc; therefore, no change in membrane order was detected. All results are the mean ± standard deviation (σ) from at least three independent experiments.

to the membrane decreases the mobility of the membrane near the headgroup region. Furthermore, at a mixing ratio of 1.5, where CBDs begin to form, and no protein binding was previously detected in Chol/POPC membranes (see Figs. 1A, 1B), there was no significant change ($P \leq 0.05$) in mobility with the addition of WT- or Q147E-αAc. A similar trend can further be seen in Figures 3C and 3D, where the samples that previously displayed protein binding to Chol/SM* membranes, WT- (see Fig. 3C) and Q147E-αAc (see Fig. 3D) with 0 mol% Chol and Q147E-αAc with 33 mol% Chol (see Fig. 3D), displayed statistically significant decreases ($P \leq 0.05$) in membrane mobility with protein binding. Additionally, in the Chol/SM* membranes sample where no protein binding was detected (see Figs. 1C, 1D), which were WT-αAc with 33 mol% Chol and Q147E-αAc with 60 mol% Chol, there were no significant changes ($P > 0.05$) to membrane mobility with the addition of protein. Relatedly, in all Chol/POPC and Chol/SM* membranes, the higher the MMSO of WT- or Q147E-αAc, the more significant the reduction in membrane mobility was with protein binding. Therefore, in both POPC and SM* membranes, the most pronounced changes in membrane mobility were seen with protein binding in the absence of Chol (0 mol%) and as less WT- or Q147E-αAc bound with the membrane with each increase in the Chol concentration, the ability of WT- or Q147E-αAc to bind and decrease the mobility near the headgroup regions was continuously reduced. Additionally, in the absence of either WT- or Q147E-αAc, there is a continuous and significant decrease ($P \leq 0.05$) in the mobility of both membranes (Chol/POPC or Chol/SM*) with each increase in Chol content. Moreover, at all Chol concentrations, the Chol/POPC membranes have significantly higher mobility parameter values than that of Chol/SM* membranes. Therefore, Chol/POPC membranes tend to form more mobile membranes than Chol/SM* membranes, and the addition of Chol both reduces the mobility of protein-free membranes and diminishes the ability of WT- and Q147E-αAc to bind and further reduce membrane mobility near the headgroup region.

Membrane Order Near the Headgroup Region of Chol/POPC and Chol/SM* Membranes With WT and Q147E αAc Binding

Shown in Figures 4A to 4D are the maximum splitting profiles, a measure of membrane order near the headgroup region, of the Chol/POPC and Chol/SM* membranes plot-

Investigative Ophthalmology & Visual Science

ted as a function of either WT- or Q147E-αAc concentration. At a Chol/lipid mixing ratio of 0 and 0.5, the binding of both WT- and Q147E-αAc generally resulted in significant increases ($P \leq 0.05$) in order near the headgroup regions for both Chol/POPC (see Figs. 4A, 4B) and Chol/SM* (see Figs. 4C, 4D) membranes. The only exceptions to this trend were for Q147E-αAc with Chol-free POPC membranes (see Fig. 4B), where there was still an apparent increase in membrane order that was significant with a $P \leq 0.1$ ($P = 0.0792$) and for WT-αAc with 33 mol% Chol containing SM* membranes where there were no significant changes ($P > 0.05$) in maximum splitting as there was no binding detected (see Fig. 1C). Similarly, for both Chol/POPC and Chol/SM* membranes at a mixing ratio of 1.5, no protein binding was detected for WT- or Q147E-αAc, and, in turn, the addition of either protein did not result in any significant change to the membrane order near the headgroup region. Last, in the protein-free control Chol/POPC and Chol/SM* membranes, with each increase in Chol concentration, there were significant increases ($P \leq 0.05$) in maximum splitting values. Furthermore, the Chol/SM* membranes showed higher maximum splitting values (more order) than the Chol/POPC membranes at all Chol concentrations. Therefore, the SM*/Chol membranes tend to form more ordered membranes than the Chol/POPC membranes, and the addition of Chol plus the formation of CBDs both increases the order of protein-free membranes and diminishes the ability of WT- and Q147E-αAc to bind and further increase membrane order near the headgroup region.

Hydrophobicity Near the Headgroup Region of POPC/Chol and SM*/Chol Membranes With WT and Q147E αAc Binding

Displayed in Figures 5A to 5D is the hydrophobicity near the headgroup regions of Chol/POPC and Chol/SM* membranes with and without WT- or Q147E-αAc. For POPC (see Figs. 5A, 5B) and SM* (see Figs. 5C, 5D) membranes without Chol, there was a significant increase ($P \leq 0.05$) in hydrophobicity near the headgroup region with both WT- and Q147E-αAc membrane binding. Additionally, the binding of WT-αAc to Chol/POPC membranes (see Fig. 5A) and Q147E-αAc to Chol/SM* (see Fig. 5D) membranes with a mixing ratio of 0.5 resulted in a significant increase ($P \leq 0.05$) in hydrophobicity near the membrane surface. Conversely, at a mixing ratio of 0.5, there was no significant change ($P > 0.05$) in hydrophobicity with WT-αAc binding to Chol/SM* (see Fig. 5C) membranes or with Q147E-αAc binding to Chol/POPC membranes (see Fig. 5B). Moreover, at a mixing ratio of 1.5 there was no significant change in hydrophobicity near the headgroup region of Chol/POPC or Chol/SM* membranes with the addition of WT- or Q147E-αAc (see Figs. 5A–D). As these increases in hydrophobicity are generally most significant in samples that displayed the most protein binding (see Figs. 1A–D), these data indicate that WT- and Q147E-αAc membrane binding is likely done through hydrophobic interactions, which is in agreeance with our previous studies showing the membrane binding of native bovine αABc and recombinant human αAc, αBc, and αABc is done via hydrophobic interactions.[5,55,59,60,63] Furthermore, independent of the addition of protein, the hydrophobicity near the headgroup region of the Chol/POPC and Chol/SM* membranes significantly decreased ($P \leq 0.05$) with each increase in Chol

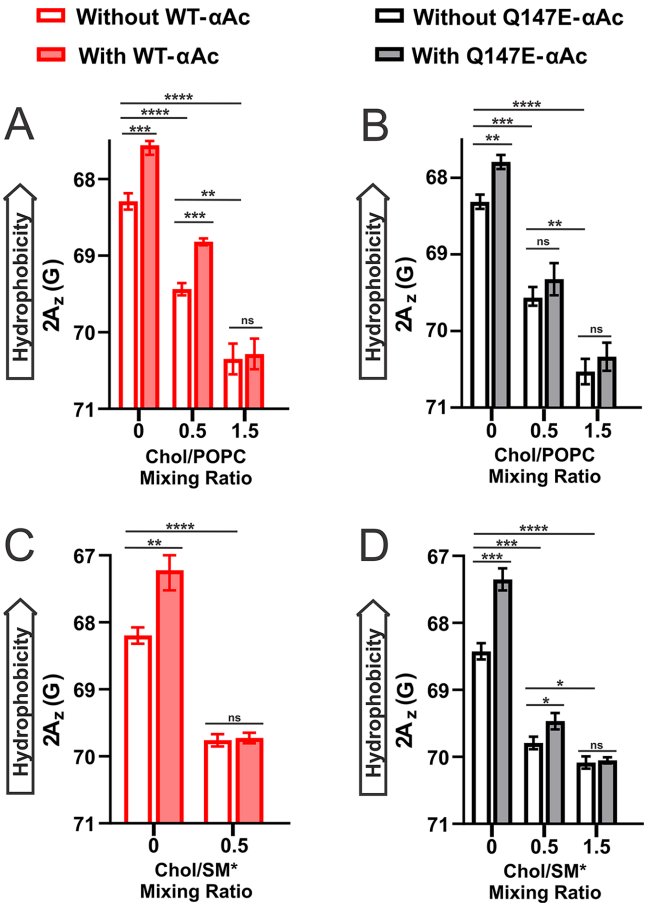

Figure 5. Hydrophobicity values near the headgroup region of Chol/POPC and Chol/SM* membrane with a Chol/lipid mixing ratio of 0 (0 mol% Chol), 0.5 (33 mol% Chol), and 1.5 (60 mol% Chol). All Chol/POPC measurements are done with (*filled*) and without (*open*) approximately 18 µM WT- or Q147E-αAc, whereas Chol/SM* measurements were taken with (*filled*) and without (*open*) approximately 54 µM WT- or Q147E-αAc. All EPR measurements were taken at −163°C to obtain a $2A_z$ value, which is inversely related to hydrophobicity, and in turn, a decrease in $2A_z$ indicates an increase in hydrophobicity. As shown in **A** to **D**, in Chol/POPC and Chol/SM* membranes, each increase in Chol content significantly decreased membrane hydrophobicity between protein-free controls. Moreover, the membrane binding of WT- and Q147E-αAc to Chol/POPC membranes (**A** and **B**) at mixing ratios of 0 and 0.5 resulted in significant increases to membrane hydrophobicity, with the binding of Q147E-αAc at a mixing ratio of 0.5 being the only exception and not displaying any significant increase in hydrophobicity with membrane binding. Additionally, as depicted in **C** and **D**, the membrane binding of WT- and Q147E-αAc to Chol/SM* membranes at mixing ratios of 0 and 0.5 resulted in significant increases in membrane hydrophobicity, except for WT-αAc at a mixing ratio of 0.5 where there was not any significant increase in hydrophobicity as there was not binding detected with the addition of protein. Lastly, for both WT- and Q147E-αAc binding with Chol/POPC and Chol/SM* membranes at a mixing ratio of 1.5 (**A–D**), there was no protein binding detected, and, in turn, there was no significant change in hydrophobicity detected with the addition of protein. All values and error bars are calculated from the average of three independent experiments. *, **, ***, and **** represents a P value < 0.05, < 0.01, < 0.001, and < 0.0001, respectively, whereas "ns" means not significant.

concentration as the addition of Chol is likely creates separation between each membrane's polar headgroups, allowing for increased water penetration. Ultimately, these trends in hydrophobicity may explain why the addition of Chol reduces the membrane binding of WT- and Q147E-αAc, as the reduction in hydrophobicity with increased Chol may reduce each membrane's capacity for hydrophobic interactions with WT- and Q147E-αAc and in turn diminish protein binding.

Discussion

As shown in Figure 6, the major findings of this study revealed that WT- and Q147E-αAc can bind to both Chol/POPC and Chol/SM* membranes, and this binding is differentially modulated by both Chol and lipid composition. Specifically, deamidation increases αAc POPC membrane binding, decreases αAc SM* membrane binding, and provides resistance to Chol inhibition, but independent of lipid composition and deamidation, high Chol and CBD content inhibits αAc and deamidated αAc binding, likely protecting against light scattering and cataract formation (see Fig. 6). These variances in binding are likely due to the alterations in αAc structure and oligomerization that occur with Q147E deamidation, where the introduction of a negative charge with Q147E deamidation has shown to reduce the β-sheet content and disrupt the hydrophobic core of αAc.[44] With these alterations, we found there are distinct changes in αAc oligomerization, where we previously found WT-αAc has an average R_h of 8.18 ± 0.48 nm and a %PD of 15.74 ± 5.03%,[5] whereas, in this study, we found Q147E-αAc has an average R_h of 7.925 ± 0.47 nm and a %PD of 21.09 ± 5.28%, meaning Q147E deamidation results in αAc forming smaller and more polydisperse oligomers.[5,75,76] These variations in αAc oligomerization likely explain the trends in MMSO, where to the Chol free-POPC membranes, the smaller Q147E-αAc oligomers may occupy less space on the membrane surface, allowing for an increased number of Q147E-αAc oligomers to bind the membrane (see Fig. 6). Interestingly, whereas the SM* membranes contain 20 mol% POPS, a negatively charged lipid, in control experiments done with only POPS membranes, we found there was no significant difference ($P > 0.05$) in the membrane binding of WT- and Q147E-αAc to POPS membranes (see Figs. 1C–E, 2E). Therefore, the possible electrostatic interactions between the negatively charged POPS and negatively charged Q147E mutant does not influence the membrane binding of αAc; however, the negatively charged POPS headgroups may repel each other,[59,61] exposing the hydrophobic core of the membrane, resulting in

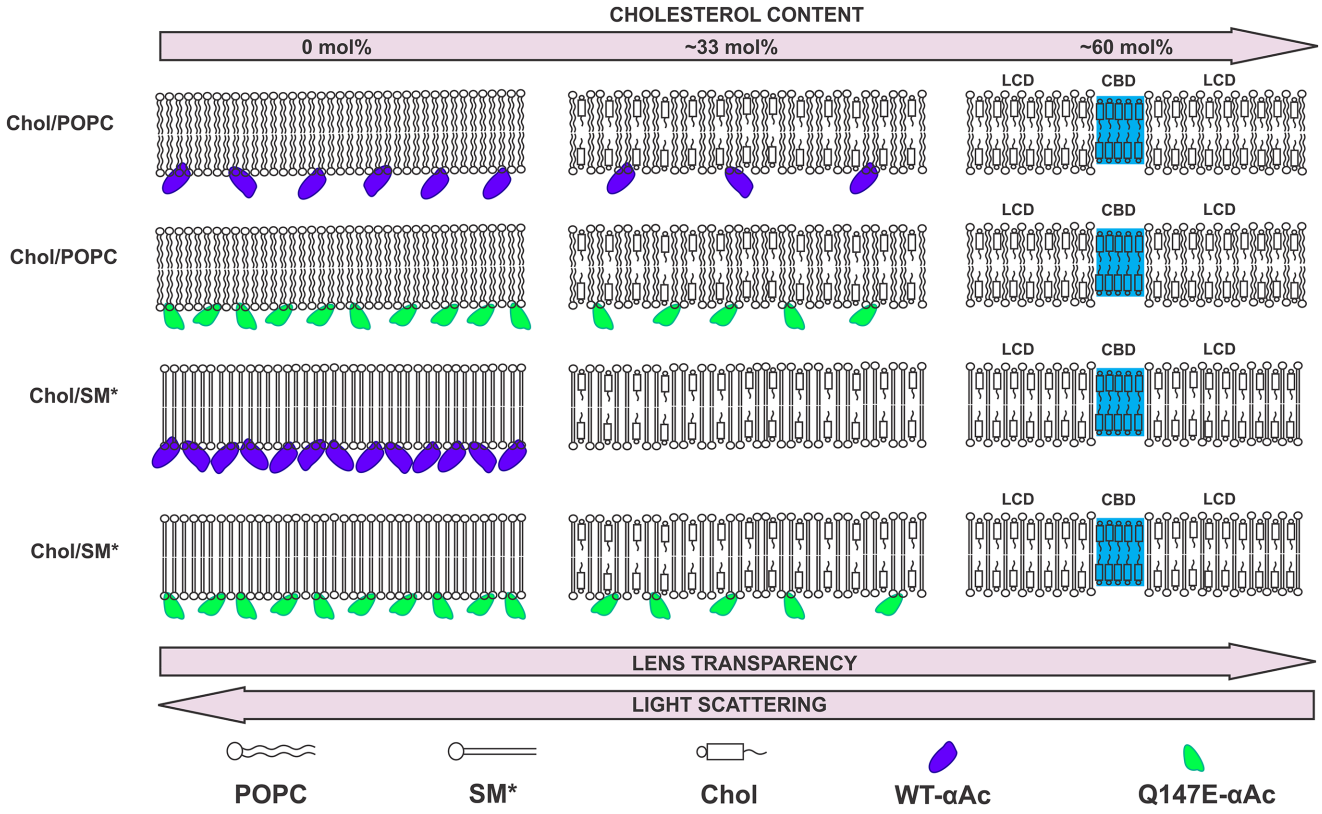

Figure 6. Schematic depicting the binding of WT- and Q147E-αAc to Chol/POPC and Chol/SM* membranes containing Chol contents of 0, 33, and 60 mol%. Compared to WT-αAc (*dark blue*), the Q147E-αAc (*green*) had increased binding to POPC and decreased binding to SM* membranes without Chol. With an increase in Chol content to 33 mol%, the membrane begins to saturate with Chol, resulting in the diminished binding of WT-αAc and, to a lesser degree, Q147E-αAc to both Chol/POPC and Chol/SM* membranes. Furthermore, with the addition of 60 mol% Chol, the membrane becomes saturated with Chol, leading to the formation of lipid cholesterol domains (LCDs) and cholesterol bilayer domains (CBDs), which completely inhibited both WT- and Q147E-αAc binding to the Chol/POPC and Chol/SM* membranes. As displayed by the *bottommost arrows*, this inhibited αAc membrane binding with increasing Chol content allows for increased lens transparency while the increased membrane binding of αAc leads to increasing levels of light scattering as seen with cataract formation. The sizes of WT- and Q147E-αAc oligomers pictured in Figure 6 are significantly larger than displayed in the schematic.

Investigative Ophthalmology & Visual Science

Table. Chol/Lipid Molar Ratios in Human Lens of Different Age Groups

	Transparent Human Lenses				Cataractous Human Lenses
Age groups	0–20 y	21–40 y	41–60 y	61–70 y	61–70 y
Chol/lipid molar ratios*					
Cortex	0.63	1.01	1.38	1.8	1.14
Nucleus	0.71	1.21	2.1	4.4	1.45

* Values were taken from references 54, 64, and 81.

the increased hydrophobic binding of WT and Q147E-αAc with the Chol-free POPS membranes compared with Chol-free SM* and POPC membranes (see Fig. 1E). In turn, the variances in SM* membrane binding are likely primarily due to the variations in αAc structure and oligomerization that occur with Q147E deamidation. These results provide us with novel insight into the need for the sharp increase in SL content and significant decrease in PC content that occurs with aging from approximately 5 years old to approximately 40 years old,[47] in which, in addition to the increasing SL content making the eye lens resistant to oxidation,[14,56–58] it may also be an evolutionary mechanism to prevent αAc membrane binding as it accumulates deamidation throughout life.

Along with lipid composition, WT- and Q147E-αAc binding is also modulated by and inversely related to the membrane Chol content. Interestingly, the interaction of WT and Q147E-αAc with Chol/SM* membrane with 33 mol% Chol differ significantly. The MMSO and K_a of WT-αAc are zero, indicating no binding of WT-αAc with Chol/SM* membrane at a mixing ratio of 0.5 (see Figs. 1C, 2C). In contrast, there is an increased binding and K_a of Q147E-αAc with 33 mol% Chol containing Chol/SM* membrane compared to WT- αAc (see Figs. 1D, 2D). These suggest strong of interaction of Q147E-αAc with biphasic membrane likely formed at Chol/SM* mixing ratio of 0.5 where the raft phase might be formed predominantly with more ordered SM membrane and Chol and non-raft phase might form with predominantly less ordered POPS and Chol membrane,[13,77–80] as SM* consists of 80% SM and 20% POPS lipid and SM forms increasingly ordered membranes compared to POPS.[61] The interaction of Q147E-αAc to the possible biphasic Chol/SM* membrane might result from the smaller oligomeric size and possible structural changes due to deamidation. However, with the formation of CBDs at 60 mol% Chol,[5,59,60,65,66] the membrane binding of WT- and Q147E-αAc to Chol/POPC and Chol/SM* membranes became completely inhibited, showing even with the increased resistance to the inhibitory effects of Chol that Q147E deamidation provides, the formation of CBDs at high Chol content[5,59,60,65,66] consistently inhibits αAc membrane binding.

These binding results show the importance of the lens Chol content changes that occur with aging where there is a significant increase in Chol/lipid ratio in transparent lenses cortical and nuclear membranes with increasing age from young (approximately 0–20 and approximately 21–40 years old) to middle-aged (approximately 41–60 years old) to old (approximately 61–70 years old) lens fiber cell membranes (see the Table).[54,64,81] However, there is a significant decrease in Chol/lipid content in the age-matched (61–70 years old) cataractous cortical and nuclear membranes compared to age-matched transparent lenses (see the Table).[54] In addition to the Chol content changing with age, the deamidation of lens crystallin has been reported to increase with both age and cataracts.[32] Specifically, it has been shown that the αAc become increasingly acidic likely due to deamidation in the lenses of 54 to 55 year old compared with fetal lenses,[82] deamidation of αAc in 26-, 34-, and 46-year-old donors increases with aging, and the percent deamidation of αAc significantly increases in the high molecular weight protein lens fractions.[83] Furthermore, the analysis of 70-year-old transparent, 70-year-old nuclear cataractous, and 93-year-old cataractous lenses were found to have increased αAc deamidation in the water-insoluble lens protein fractions compared to the water-soluble fraction.[33] In addition to deamidation occurring at increasing rates among these insoluble protein fractions, it has also been reported that water-insoluble crystallins in young, aged, and cataractous human lenses are membrane-bound.[8] Therefore, with cataract formation, the Chol content of both the cortex and nucleus significantly decreases, PC content decreases, and SM content increases, whereas αAc simultaneously shows to become increasingly deamidated, insoluble, and membrane-bound.[8,54,81,82,84] Based on these previous discoveries and the findings from this study, it appears the formation of CBDs is needed to prevent the binding of αAc and deamidated αAc to the lens membrane (see Fig. 6) and the formation of large membrane-αAc aggregates responsible for scattering light, however, with the loss of Chol, CBDs, and lipid rafts found in cataract development,[54] paired with the increasing rates of deamidation, αAc is likely no longer inhibited from binding to the lens membrane, explaining why there is the accumulation of deamidated αAc in the insoluble pellets of aged lenses.[6,8,14,38,45,46,85,86] In turn, it appears that the eye lens lipid and Chol composition changes generally coincide with the modification of α-crystallin and, therefore, may be an evolutionary mechanism to not only prevent lens membrane oxidation[14,56–58] but also promote lipid raft and CBDs formation[13,77–80,87] and prevent the membrane binding of αAc as it becomes increasingly modified.

Relatedly, although a Chol/lipid mixing ratio around 1.5 was enough to inhibit the binding of αAc in this study, and therefore even the reduced cataractous lens Chol levels (see the Table) would likely have a similar effect, the concentration of αAc in this study reaches a maximum of approximately 1.1 mg/mL, whereas αABc concentration in the human lens has been estimated to reach approximately 140 to 158 mg/mL, whereas αABc comprised of approximately 75% αAc.[15,40] Therefore, with the significant increase in αABc concentration relative to the amount used in this study, it is likely more αAc is interacting with and able to bind to the reduced Chol-containing cataractous lens membrane. Moreover, this study is only done with one site of deamidation while αAc has shown to accumulate multiple sites of modification,[33,75,82,84] which can likely further exemplify the results found in this study and promote αAc membrane binding at even higher Chol levels. Furthermore, it has been reported that lens lipid and Chol undergo extensive oxida-

Investigative Ophthalmology & Visual Science

tion with age and cataract formation,[88–91] which has shown to reduce the overall membrane Chol content.[92–96] Relatedly, genetic mutations in rats that decrease lens Chol to approximately 57% of the normal levels of healthy rats have been found to result in the formation of cataracts,[97] whereas other in vivo studies report that the knockout of lens Chol production results in the development of cataracts.[67] Therefore, both lens oxidation and genetic deficiencies in the human lens Chol biosynthesis pathways that reduce lens Chol levels likely allow for even more pronounced αAc membrane binding and the accumulation of deamidated crystallins in the membrane and insoluble pellets of aged lenses. Therefore, as a whole, it appears the continual increase in the lens SM and Chol content found with normal aging[13,14,26,55,59,63,64] is crucial for preventing the accumulation of membrane-bound αAc, especially as αAc becomes increasingly resistant to the effects of Chol due to the accumulation of deamidation (see Fig. 6). Furthermore, the loss of membrane Chol due to factors such as membrane oxidation and genetic deficiencies in the production of lens Chol could lead to crystallin/modified crystallin-membrane binding followed by the formation of large aggregates responsible for light scattering and development of age-related and early-onset cataract (see Fig. 6).

As displayed in Figures 2A to 2D, WT- and Q147E-αAc each had the highest K_a with Chol-free POPC membranes, but with each increase in Chol concentration, the affinity of both WT- and Q147E-αAc significantly decreased ($P \leq 0.05$) until neither protein had any affinity with 60 mol% Chol. Additionally, whereas the K_a trends of WT- and Q147E-αAc in Chol/POPC membranes with increasing concentrations of Chol were consistent, in Chol/SM* membranes, there was a substantial deviation in trend with the addition of Chol. Specifically, in Chol/SM* membranes at a mixing ratio of 0.5, Q147E-αAc was the only sample that displayed an increase in K_a, whereas WT-αAc was the only sample with no membrane affinity. Interestingly, in our control POPS studies, the K_a of Q147E was lower than WT to POPS membranes (see Figs. 2E, 2F), indicating there is a synergistic effect between the hydrophobic interactions of the structurally altered Q147E-αAc and the multiple membrane phases of the 33 mol% Chol-containing SM* membranes. However, although not analyzed for WT-αAc as it already showed no affinity for Chol/SM* membranes at a mixing ratio of 0.5, with the formation of CBDs at 60 mol% Chol Q147E-αAc did not display any membrane affinity.[5,59,60,65,66] Therefore, the addition of Chol seems to have similar effects on both WT- and Q147E-αAc in Chol/POPC membranes, generally lowering membrane affinity with increasing Chol concentrations, but has more variance on WT- and Q147E-αAc binding in Chol/SM* membranes, likely due to the increased membrane order and formation of lipid rafts in Chol/SM* membranes.[13,77–80,98–100] However, regardless of lipid type with the formation of CBDs at high Chol content,[5,59,60,65,66] both WT and Q147E-αAc no longer have any membrane affinity. Therefore, these results indicate that the reduction of Chol and CBDs in cataractous lenses[54,101,102] likely promotes αAc lens membrane binding, especially as αAc becomes increasingly modified, making the increase in lens Chol and CBD content with healthy aging a crucial mechanism for depleting αAc membrane affinity and preventing the lens binding of both WT and modified αAc.[33,85,86,103–108]

As displayed in Figures 3 and 4A to 4D, the membrane lipid/Chol composition and the membrane binding of WT- and Q147E-αAc also alter the physical properties of the Chol/POPC and Chol/SM* membranes. Specifically, WT- and Q147E-αAc membrane binding significantly ($P \leq 0.05$) decreases the mobility and increases the order of Chol/POPC and Chol/SM* membranes near the headgroup region. Moreover, these physical changes appear to be directly related to MMSO, with increased membrane binding inducing more significant changes in membrane mobility and order. In addition to protein binding affecting membrane mobility, adding Chol also directly reduced membrane mobility while increasing the order near the headgroup region of protein-free control membranes. Therefore, altogether, these data indicate that an increased Chol content both decreases membrane mobility and increases membrane order near the headgroup region while diminishing the ability of αAc to bind and further alter membrane mobility and order of both Chol/POPC and Chol/SM* membranes.

Last, our results also show that WT- and Q147E-αAc membrane binding increases the hydrophobic environment near the headgroup region of both the Chol/POPC and Chol/SM* membranes, indicating this binding is likely done through hydrophobic interactions. Moreover, the addition of Chol significantly decreases protein-free control membrane surface hydrophobicity and diminishes the hydrophobic membrane binding of WT- and Q147E-αAc. This reduced hydrophobicity with the addition of Chol is likely due to Chol separating the polar lipid headgroups in each membrane, allowing for increased water penetration at the surface of the membrane and, in turn, reducing the hydrophobicity of the environment near the membrane surface. Additionally, as the membrane binding of both WT- and Q147E-αAc is likely done through hydrophobic interactions, their membrane binding may form a hydrophobic barrier on the membrane surface for the diffusion of small molecules, such as glutathione, in turn, creating an oxidative environment within the lens that promotes cataract development.[5,55,59,60,62,63] Moreover, as Q147E deamidation provides increased resistance to the inhibitory effect of Chol, the accumulation of deamidation in αAc throughout life may promote this hydrophobic lens binding and increase the likelihood of developing such hydrophobic barriers. Therefore, these results suggest that the increases in lens Chol and CBD content found with healthy aging[13,14,26,55,59,63,64] is a critical mechanism needed to inhibit these hydrophobic crystallin interactions with the lens membrane and prevent the formation of a hydrophobic barrier and cataracts. In contrast, the significant decrease in the lens Chol content found with cataract development[54,101,102] likely increases the lens susceptibility for the formation of such hydrophobic barriers and the progression of cataracts.

The results discussed in this study are in agreeance with our previous studies, where we found both recombinant human αAc, αBc, αABc,[5] and native bovine lens αABc[55,59–63] can bind through hydrophobic interactions with individual lipid membranes,[59,61,62] model lens lipid membranes,[60] and membranes made from extracted cortical and nuclear lipids of single bovine[63] or human lenses[55] and appears to be strongly modulated by the membrane's lipid and Chol content.[5,59,61–63] To add to these works, in this study, we are the first to find that age-related lens lipid changes may be a necessary evolutionary mechanism to not only make the lens resistant to oxidation,[14,56–58] but also diminish the binding of αAc as it accumulates deamidation throughout life.[4,7,19,29,33,42]

Acknowledgments

Supported by the National Eye Institute (NEI) and the National Institute of General Medical Sciences (NIGMS) branch of the National Institutes of Health (NIH) under the Award Number R01EY030067 via IDeA co-funding.

The content of this manuscript is solely the responsibility of the authors and is not necessarily representative of the National Institutes of Health's official views.

Disclosure: **P. Hazen**, None; **N.K. Khadka**, None; **L. Mainali**, None

References

1. De Bruyne S, van Schie L, Himpe J, et al. A potential role for fructosamine-3-kinase in cataract treatment. *Int J Mol Sci*. 2021;22(8):3841.
2. Hains PG, Truscott RJW. Post-translational modifications in the nuclear region of young, aged, and cataract human lenses. *J Proteome Res*. 2007;6(10):3935–3943.
3. Takata T, Oxford JT, Demeler B, Lampi KJ. Deamidation destabilizes and triggers aggregation of a lens protein, βA3-crystallin. *Protein Sci Publ Protein Soc*. 2008;17(9):1565–1575.
4. Lampi KJ, Amyx KK, Ahmann P, Steel EA. Deamidation in human lens βB2-crystallin destabilizes the dimer. *Biochemistry*. 2006;45(10):3146–3153.
5. Timsina R, Hazen P, Trossi-Torres G, Khadka NK, Kalkat N, Mainali L. Cholesterol content regulates the interaction of αA-, αB-, and α-crystallin with the model of human lens-lipid membranes. *Int J Mol Sci*. 2024;25(3):1923.
6. Datales MB, 3rd, Ansari RR, Yoshida J, et al. Longitudinal study of age-related cataract using dynamic light scattering: loss of α-crystallin leads to nuclear cataract development. *Ophthalmology*. 2016;123(2):248–254.
7. Takata T, Oxford JT, Lampi KJ. Deamidation alters the structure and decreases the stability of human lens βA3-crystallin. *Biochemistry*. 2007;46(30):8861–8871.
8. Chandrasekher G, Cenedella RJ. Protein associated with human lens 'native' membrane during aging and cataract formation. *Exp Eye Res*. 1995;60(6):707–717.
9. Horwitz J, Bova MP, Ding LL, Haley DA, Stewart PL. Lens α-crystallin: function and structure. *Eye*. 1999;13(3):403–408.
10. Rocha MA, Sprague-Piercy MA, Kwok AO, Roskamp KW, Martin RW. Chemical properties determine solubility and stability in βγ-crystallins of the eye lens. *Chembiochem*. 2021;22:1329–1346.
11. Hejtmancik JF, Riazuddin SA, McGreal R, Liu W, Cvekl A, Shiels A. Lens biology and biochemistry. *Prog Mol Biol Transl Sci*. 2015;134:169–201.
12. Michiel M, Duprat E, Skouri-Panet F, et al. Aggregation of deamidated human βB2-crystallin and incomplete rescue by α-crystallin chaperone. *Exp Eye Res*. 2010;90(6):688–698.
13. Hazen P, Trossi-Torres G, Khadka NK, Timsina R, Mainali L. Binding of βL-crystallin with models of animal and human eye lens-lipid membrane. *Int J Mol Sci*. 2023;24(17):13600.
14. Timsina R, Mainali L. Association of alpha-crystallin with fiber cell plasma membrane of the eye lens accompanied by light scattering and cataract formation. *Membranes*. 2021;11(6):447.
15. Horwitz J. Alpha-crystallin. *Exp Eye Res*. 2003;76(2):145–153.
16. Sharma KK, Santhoshkumar P. Lens aging: effects of crystallins. *Biochim Biophys Acta BBA - Gen Subj*. 2009;1790(10):1095–1108.
17. Srinivas P, Narahari A, Petrash JM, Swamy MJ, Reddy GB. Importance of eye lens α-crystallin heteropolymer with 3:1 αA to αB ratio: stability, aggregation, and modifications. *IUBMB Life*. 2010;62(9):693–702.
18. Moffat BA, Landman KA, Truscott RJW, Sweeney MHJ, Pope JM. Age-related changes in the kinetics of water transport in normal human lenses. *Exp Eye Res*. 1999;69(6):663–669.
19. Srivastava OP, Srivastava K, Silney C. Levels of crystallin fragments and identification of their origin in water soluble high molecular weight (HMW) proteins of human lenses. *Curr Eye Res*. 1996;15(5):511–520.
20. Cobb BA, Petrash JM. Characterization of α-crystallin-plasma membrane binding. *J Biol Chem*. 2000;275(9):6664–6672.
21. Srivastava K, Chaves JM, Srivastava OP, Kirk M. Multi-crystallin complexes exist in the water-soluble high molecular weight protein fractions of aging normal and cataractous human lenses. *Exp Eye Res*. 2008;87(4):356–366.
22. Harrington V, Srivastava OP, Kirk M. Proteomic analysis of water insoluble proteins from normal and cataractous human lenses. *Mol Vis*. 2007;13:1680–1694.
23. Santhoshkumar P, Raju M, Sharma KK. αA-crystallin peptide SDRDKFVIFLDVKHF accumulating in aging lens impairs the function of α-crystallin and induces lens protein aggregation. *PLoS One*. 2011;6(4):e19291.
24. Delbecq SP, Klevit RE. One size does not fit all: the oligomeric states of αB crystallin. *FEBS Lett*. 2013;587(8):1073–1080.
25. Sprague-Piercy MA, Rocha MA, Kwok AO, Martin RW. α-Crystallins in the vertebrate eye lens: complex oligomers and molecular chaperones. *Annu Rev Phys Chem*. 2021;72:143–163.
26. Khadka NK, Hazen P, Haemmerle D, Mainali L. Interaction of βL- and γ-crystallin with phospholipid membrane using atomic force microscopy. *Int J Mol Sci*. 2023;24(21):15720.
27. Srivastava OP, Srivastava K, Chaves JM, Gill AK. Post-translationally modified human lens crystallin fragments show aggregation in vitro. *Biochem Biophys Rep*. 2017;10:94–131.
28. Takata T, Woodbury LG, Lampi KJ. Deamidation alters interactions of beta-crystallins in hetero-oligomers. *Mol Vis*. 2009;15:241–249.
29. Su SP, McArthur JD, Friedrich MG, Truscott RJW, Aquilina JA. Understanding the α-crystallin cell membrane conjunction. *Mol Vis*. 2011;17:2798–2807.
30. Bateman OA, Sarra R, Van Genesen ST, Kappé G, Lubsen NH, Slingsby C. The stability of human acidic β-crystallin oligomers and hetero-oligomers. *Exp Eye Res*. 2003;77(4):409–422.
31. Truscott RJW, Comte-Walters S, Ablonczy Z, et al. Tight binding of proteins to membranes from older human cells. *Age*. 2011;33(4):543–554.
32. Hains PG, Truscott RJW. Age-dependent deamidation of lifelong proteins in the human lens. *Invest Ophthalmol Vis Sci*. 2010;51(6):3107–3114.
33. Wilmarth PA, Tanner S, Dasari S, et al. Age-related changes in human crystallins determined from comparative analysis of post-translational modifications in young and aged lens: does deamidation contribute to crystallin insolubility? *J Proteome Res*. 2006;5(10):2554–2566.
34. Feng J, Smith DL, Smith JB. Human lens β-crystallin solubility. *J Biol Chem*. 2000;275(16):11585–11590.
35. Gupta R, Srivastava K, Srivastava OP. Truncation of motifs III and IV in human lens βA3-crystallin destabilizes the structure. *Biochemistry*. 2006;45(33):9964–9978.
36. Liu BF, Liang JJN. Protein–protein interactions among human lens acidic and basic β-crystallins. *FEBS Lett*. 2007;581(21):3936–3942.

Investigative Ophthalmology & Visual Science

37. Chandrasekher G, Cenedella RJ. Protein associated with human lens "native" membrane during aging and cataract formation. *Exp Eye Res*. 1995;60(6):707–717.
38. Friedrich MG, Truscott RJW. Large-scale binding of α-crystallin to cell membranes of aged normal human lenses: a phenomenon that can be induced by mild thermal stress. *Invest Ophthalmol Vis Sci*. 2010;51(10):5145–5152.
39. Cobb BA, Petrash JM. alpha-Crystallin chaperone-like activity and membrane binding in age-related cataracts. *Biochemistry*. 2002;41(2):483–490.
40. Moreau KL, King JA. Protein misfolding and aggregation in cataract disease and prospects for prevention. *Trends Mol Med*. 2012;18(5):273–282.
41. Zhao L, Chen XJ, Zhu J, et al. Lanosterol reverses protein aggregation in cataracts. *Nature*. 2015;523(7562):607–611.
42. Li X, Lin C, O'Connor PB. Glutamine deamidation: differentiation of glutamic acid and γ-Glutamic acid in peptides by electron capture dissociation. *Anal Chem*. 2010;82(9):3606–3615.
43. Searle BC, Dasari S, Wilmarth PA, et al. Identification of protein modifications using MS/MS de novo sequencing and the OpenSea alignment algorithm. *J Proteome Res*. 2005;4(2):546–554.
44. Ray NJ, Hall D, Carver JA. A structural and functional study of Gln147 deamidation in αA-crystallin, a site of modification in human cataract. *Exp Eye Res*. 2017;161:163–173.
45. Boyle DL, Takemoto L. EM immunolocalization of alpha-crystallins: association with the plasma membrane from normal and cataractous human lenses. *Curr Eye Res*. 1996;15(5):577–582.
46. Cenedella RJ, Fleschner CR. Selective association of crystallins with lens "native" membrane during dynamic cataractogenesis. *Curr Eye Res*. 1992;11(8):801–815.
47. Grami V, Marrero Y, Huang L, Tang D, MC Yappert, Borchman D. α-Crystallin binding in vitro to lipids from clear human lenses. *Exp Eye Res*. 2005;81(2):138–146.
48. Tang D, Borchman D, Yappert MC, Cenedella RJ. Influence of cholesterol on the interaction of α-crystallin with phospholipids. *Exp Eye Res*. 1998;66(5):559–567.
49. Chandrasekher G, Cenedella RJ. Properties of α-crystallin bound to lens membrane: probing organization at the membrane surface. *Exp Eye Res*. 1997;64(3):423–430.
50. Borchman D, Tang D. Binding capacity of α-crystallin to bovine lens lipids. *Exp Eye Res*. 1996;63(4):407–410.
51. Sato H, Borchman D, Ozaki Y, et al. Lipid –protein interactions in human and bovine lens membranes by fourier transform raman and infrared spectroscopies. *Exp Eye Res*. 1996;62(1):47–54.
52. Tang D, Borchman D, Yappert MC. Alpha-crystallin/lens lipid interactions using resonance energy transfer. *Ophthalmic Res*. 1999;31(6):452–462.
53. Cobb BA, Petrash JM. Factors influencing alpha-crystallin association with phospholipid vesicles. *Mol Vis*. 2002;8:85–93.
54. Mainali L, Raguz M, O'Brien WJ, Subczynski WK. Properties of membranes derived from the total lipids extracted from clear and cataractous lenses of 61-70-year-old human donors. *Eur Biophys J EBJ*. 2015;44(1-2):91–102.
55. Hazen P, Trossi-Torres G, Timsina R, Khadka NK, Mainali L. Association of alpha-crystallin with human cortical and nuclear lens lipid membrane increases with the grade of cortical and nuclear cataract. *Int J Mol Sci*. 2024;25(3):1936.
56. Deeley JM, Mitchell TW, Wei X, et al. Human lens lipids differ markedly from those of commonly used experimental animals. *Biochim Biophys Acta*. 2008;1781(6-7):288–298.
57. Borchman D, Yappert MC, Afzal M. Lens lipids and maximum lifespan. *Exp Eye Res*. 2004;79(6):761–768.
58. Borchman D, Stimmelmayr R, George JC. Whales, lifespan, phospholipids, and cataracts. *J Lipid Res*. 2017;58(12):2289–2298.
59. Timsina R, Trossi-Torres G, O'Dell M, Khadka NK, Mainali L. Cholesterol and cholesterol bilayer domains inhibit binding of alpha-crystallin to the membranes made of the major phospholipids of eye lens fiber cell plasma membranes. *Exp Eye Res*. 2021;206:108544.
60. Timsina R, Trossi-Torres G, Thieme J, O'Dell M, Khadka NK, Mainali L. Alpha-crystallin association with the model of human and animal eye lens-lipid membranes is modulated by surface hydrophobicity of membranes. *Curr Eye Res*. 2022;47(6):843–853.
61. Timsina R, Khadka NK, Maldonado D, Mainali L. Interaction of alpha-crystallin with four major phospholipids of eye lens membranes. *Exp Eye Res*. 2021;202:108337.
62. Trossi-Torres G, Timsina R, Mainali L. Alpha-crystallin-membrane association modulated by phospholipid acyl chain length and degree of unsaturation. *Membranes*. 2022;12(5):455.
63. Timsina R, Wellisch S, Haemmerle D, Mainali L. Binding of alpha-crystallin to cortical and nuclear lens lipid membranes derived from a single lens. *Int J Mol Sci*. 2022;23(19):11295.
64. Mainali L, Raguz M, O'Brien WJ, Subczynski WK. Changes in the properties and organization of human lens lipid membranes occurring with age. *Curr Eye Res*. 2017;42(5):721–731.
65. Mainali L, Pasenkiewicz-Gierula M, Subczynski WK. Formation of cholesterol bilayer domains precedes formation of cholesterol crystals in membranes made of the major phospholipids of human eye lens fiber cell plasma membranes. *Curr Eye Res*. 2020;45(2):162–172.
66. Raguz M, Mainali L, Widomska J, Subczynski WK. Using spin-label electron paramagnetic resonance (EPR) to discriminate and characterize the cholesterol bilayer domain. *Chem Phys Lipids*. 2011;164(8):819–829.
67. Shin S, Zhou H, He C, et al. Qki activates Srebp2-mediated cholesterol biosynthesis for maintenance of eye lens transparency. *Nat Commun*. 2021;12(1):3005.
68. Horwitz J, Huang QL, Ding L, Bova MP. [30]Lens α-crystallin: chaperone-like properties. In: *Methods in Enzymology*. Vol. 290. Molecular Chaperones. Sam Diego, CA: Academic Press; 1998:365–383.
69. MAN0018595_BL21_DE3competent_cells_UG.pdf. Accessed December 2, 2023. Available at: https://assets.thermofisher.com/TFS-Assets/LSG/manuals/MAN0018595_BL21_DE3competent_cells_UG.pdf.
70. Gasteiger E, Hoogland C, Gattiker A, et al. Protein identification and analysis tools on the ExPASy Server. In: Walker JM, ed. *The Proteomics Protocols Handbook*. Totowa, NJ: Humana Press; 2005:571–607.
71. Buboltz JT, Feigenson GW. A novel strategy for the preparation of liposomes: rapid solvent exchange. *Biochim Biophys Acta BBA - Biomembr*. 1999;1417(2):232–245.
72. Huang J, Buboltz JT, Feigenson GW. Maximum solubility of cholesterol in phosphatidylcholine and phosphatidylethanolamine bilayers. *Biochim Biophys Acta BBA - Biomembr*. 1999;1417(1):89–100.
73. McMullen TPW, Lewis RNAH, McElhaney RN. Cholesterol–phospholipid interactions, the liquid-ordered phase and lipid rafts in model and biological membranes. *Curr Opin Colloid Interface Sci*. 2004;8(6):459–468.
74. Mainali L, O'Brien WJ, Timsina R. Interaction of alpha-crystallin with phospholipid membranes. *Curr Eye Res*. 2021;46(2):185–194.

Investigative Ophthalmology & Visual Science

75. Sharma KK, Santhoshkumar P. Lens aging: effects of crystallins. *Biochim Biophys Acta*. 2009;1790(10):1095–1108.
76. Peschek J, Braun N, Franzmann TM, et al. The eye lens chaperone α-crystallin forms defined globular assemblies. *Proc Natl Acad Sci USA*. 2009;106(32):13272–13277.
77. Edidin M. The state of lipid rafts: from model membranes to cells. *Annu Rev Biophys Biomol Struct*. 2003;32(1):257–283.
78. London E. Insights into lipid raft structure and formation from experiments in model membranes. *Curr Opin Struct Biol*. 2002;12(4):480–486.
79. Simons K, Vaz WLC. Model systems, lipid rafts, and cell membranes. *Annu Rev Biophys Biomol Struct*. 2004;33(1):269–295.
80. Subczynski WK, Pasenkiewicz-Gierula M, Widomska J, Mainali L, Raguz M. High cholesterol/low cholesterol: effects in biological membranes review. *Cell Biochem Biophys*. 2017;75(3-4):369–385.
81. Mainali L, Raguz M, O'Brien WJ, Subczynski WK. Properties of membranes derived from the total lipids extracted from the human lens cortex and nucleus. *Biochim Biophys Acta*. 2013;1828(6):1432–1440.
82. Lampi KJ, Ma Z, Hanson SR, et al. Age-related changes in human lens crystallins identified by two-dimensional electrophoresis and mass spectrometry. *Exp Eye Res*. 1998;67(1):31–43.
83. Takemoto L. Increased deamidation of asparagine-101 from alpha-A crystallin in the high molecular weight aggregate of the normal human lens. *Exp Eye Res*. 1999;68(5):641–645.
84. Ma Z, Hanson SRA, Lampi KJ, David LL, Smith DL, Smith JB. Age-related changes in human lens crystallins identified by HPLC and mass spectrometry. *Exp Eye Res*. 1998;67(1):21–30.
85. McFall-Ngai MJ, Ding LL, Takemoto LJ, Horwitz J. Spatial and temporal mapping of the age-related changes in human lens crystallins. *Exp Eye Res*. 1985;41(6):745–758.
86. Roy D, Spector A. Absence of low-molecular-weight alpha crystallin in nuclear region of old human lenses. *Proc Natl Acad Sci USA*. 1976;73(10):3484–3487.
87. Widomska J, Subczynski WK, Mainali L, Raguz M. Cholesterol bilayer domains in the eye lens health: a review. *Cell Biochem Biophys*. 2017;75(3):387–398.
88. Bhuyan KC, Bhuyan DK, Podos SM. Lipid peroxidation in cataract of the human. *Life Sci*. 1986;38(16):1463–1471.
89. Babizhayev MA. Lipid fluorophores of the human crystalline lens with cataract. *Graefes Arch Clin Exp Ophthalmol*. 1989;227(4):384–391.
90. Borchman D, Yappert MC. Age-related lipid oxidation in human lenses. *Invest Ophthalmol Vis Sci*. 1998;39(6):1053–1058.
91. Girão H, Mota MC, Ramalho J, Pereira P. Cholesterol oxides accumulate in human cataracts. *Exp Eye Res*. 1998;66(5):645–652.
92. Mainali L, Zareba M, Subczynski WK. Oxidation of polyunsaturated phospholipid decreases the cholesterol content at which cholesterol bilayer domains start to form in phospholipid-cholesterol membranes. *Biophys J*. 2017;112(3):375a.
93. Mainali L, Pasenkiewicz-Gierula M, Subczynski WK. Formation of cholesterol bilayer domains precedes formation of cholesterol crystals in membranes made of the major phospholipids of human eye lens fiber cell plasma membranes. *Curr Eye Res*. 2020;45(2):162–172.
94. Mainali L, Zareba M, Subczynski W. Oxidation of cholesterol and formation of cholesterol hydroperoxides decreases the cholesterol concentration at which formation of cholesterol bilayer domains and cholesterol crystals is initiated in phospholipid bilayers. *Biophys J*. 2016;110(3):74a.
95. Jacob RF, Aleo MD, Self-Medlin Y, Doshna CM, Mason RP. 1,2-naphthoquinone stimulates lipid peroxidation and cholesterol domain formation in model membranes. *Invest Ophthalmol Vis Sci*. 2013;54(12):7189–7197.
96. Jacob RF, Mason RP. Lipid peroxidation induces cholesterol domain formation in model membranes. *J Biol Chem*. 2005;280(47):39380–39387.
97. Mori M, Li G, Abe I, et al. Lanosterol synthase mutations cause cholesterol deficiency–associated cataracts in the Shumiya cataract rat. *J Clin Invest*. 2006;116(2):395–404.
98. Wisniewska A, Subczynski WK. The liquid-ordered phase in sphingomyelincholesterol membranes as detected by the discrimination by oxygen transport (DOT) method. *Cell Mol Biol Lett*. 2008;13(3):430–451.
99. Barba-Bon A, Nilam M, Hennig A. Supramolecular chemistry in the biomembrane. *Chembiochem*. 2020;21(7):886–910.
100. Zhu X, Gaus K, Lu Y, Magenau A, Truscott RJW, Mitchell TW. α- and β-crystallins modulate the head group order of human lens membranes during aging. *Invest Ophthalmol Vis Sci*. 2010;51(10):5162–5167.
101. Jacob RF, Cenedella RJ, Mason RP. Evidence for distinct cholesterol domains in fiber cell membranes from cataractous human lenses. *J Biol Chem*. 2001;276(17):13573–13578.
102. Widomska J, Subczynski WK. Why is very high cholesterol content beneficial for the eye lens but negative for other organs? *Nutrients*. 2019;11(5):1083.
103. Harrington V, McCall S, Huynh S, Srivastava K, Srivastava OP. Crystallins in water soluble-high molecular weight protein fractions and water insoluble protein fractions in aging and cataractous human lenses. *Mol Vis*. 2004;10:476–489.
104. Hanson SR, Hasan A, Smith DL, Smith JB. The major in vivo modifications of the human water-insoluble lens crystallins are disulfide bonds, deamidation, methionine oxidation and backbone cleavage. *Exp Eye Res*. 2000;71(2):195–207.
105. Heys KR, Friedrich MG, Truscott RJW. Presbyopia and heat: changes associated with aging of the human lens suggest a functional role for the small heat shock protein, alpha-crystallin, in maintaining lens flexibility. *Aging Cell*. 2007;6(6):807–815.
106. Aarts HJ, Lubsen NH, Schoenmakers JG. Crystallin gene expression during rat lens development. *Eur J Biochem*. 1989;183(1):31–36.
107. Su SP, McArthur JD, Truscott RJW, Aquilina JA. Truncation, cross-linking and interaction of crystallins and intermediate filament proteins in the aging human lens. *Biochim Biophys Acta*. 2011;1814(5):647–656.
108. Hoehenwarter W, Klose J, Jungblut PR. Eye lens proteomics. *Amino Acids*. 2006;30(4):369–389.

Investigative Ophthalmology & Visual Science